

# Kinetics of Emulsifier-Free Emulsion Polymerization of Methyl Methacrylate

TANER TANRISEVER,<sup>1</sup> OĞUZ OKAY,<sup>2\*</sup> and INCI ÇETİN SÖNMEZOĞLU<sup>3</sup>

<sup>1</sup>Balikesir University, Necatibey Education Faculty, Department of Chemistry Education, 10100 Balikesir, Turkey, <sup>2</sup>TUBITAK Marmara Research Center and Kocaeli University, Department of Chemistry, PO Box 21, 41470 Gebze, Kocaeli, Turkey, and <sup>3</sup>Yildiz Technical University, Department of Chemistry, 80270 Istanbul, Turkey

## SYNOPSIS

The influences of polymerization temperature, initiator and monomer concentrations, ionic strength of the aqueous phase, as well as ethylene glycol dimethacrylate (EGDM) comonomer, on the kinetics of the emulsifier-free emulsion polymerization of methyl methacrylate (MMA) and on the properties of the resulting poly(methyl methacrylate) (PMMA) lattices were studied. The polymerizations were carried out using potassium persulfate (KPS) as the initiator. Monodisperse PMMA lattices with particle diameters varying between 0.14–0.37  $\mu\text{m}$  and polymer molecular weights of the order  $0.4 \times 10^6$  to  $1.2 \times 10^6$  g/mol were prepared. The initial rate of polymerization increases with increasing temperature, KPS-MMA mole ratio, EGDM content, or with decreasing ionic strength of the aqueous phase. It was shown that the bead size can be limited by reducing the monomer concentration or by using the cross-linking agent EGDM. The ionic strength of the aqueous phase has a dominant effect on final particle diameter and polymer molecular weight. The uniformity of the latex particles increases as the temperature increases or as the initiator concentration decreases. The experimental results can be reasonably interpreted by the homogeneous nucleation mechanism of the emulsifier-free emulsion polymerization of MMA. © 1996 John Wiley & Sons, Inc.

## INTRODUCTION

In recent years, emulsion polymerization in the absence of added emulsifier has received considerable attention as a method for producing monodisperse and “clean” lattices.<sup>1–7</sup> In such a polymerization system, polymer particles are stabilized by ionizable initiators or by ionic comonomers. Several mechanisms have been proposed for particle nucleation and growth during polymerization without emulsifier.<sup>8–10</sup> It is generally agreed that the actual process depends on the water solubility of the monomer. For example, in the presence of the water-soluble initiator, potassium persulfate (KPS), it has been proposed that slightly water-soluble monomers, such as styrene, polymerize in aqueous phase to oligomeric radicals with sulfate end groups, which are

surface active and form micelles in an emulsion polymerization.<sup>8</sup> However, for more water-soluble monomers, such as (meth)acrylates, the particles are formed by the precipitation of growing chains upon achievement of a critical chain length, which is 60–80 for the monomer methyl methacrylate.<sup>10</sup> In both cases, subsequent polymerization would occur in monomer swollen particles.

Although extensive work has been reported in the literature for the emulsifier-free emulsion polymerization of styrene, only a few were concerned for methyl methacrylate (MMA) polymerization.<sup>6,11</sup> Here, we present new measurements for the emulsifier-free emulsion polymerization of MMA, which will enable us to develop a deeper insight into the phenomena occurring during the polymerization. For this purpose, a series of experiments was carried out at various reaction conditions. Monomer conversions, molecular weights, and particle sizes were investigated as a function of the polymerization temperature, monomer and initiator concentrations,

\* To whom correspondence should be addressed.

and the ionic strength of the aqueous phase, as well as the concentration of the cross-linking agent, ethylene glycol dimethacrylate.

## EXPERIMENTAL

### Materials

The monomers methyl methacrylate (MMA) and ethylene glycol dimethacrylate (EGDM) were freed from the inhibitor by shaking with 5% aqueous NaOH, washing with water, and drying over Na<sub>2</sub>SO<sub>4</sub>. They were then distilled under reduced pressure. Purity was checked by gas chromatography and found to be about 98%. The initiator, potassium persulfate, was a product of Fluka, Germany. The deionized water used for polymerization was distilled twice before use. Sodium chloride (NaCl) and potassium chloride (KCl) (both analytical grades) were used without further purification.

### Polymerization Procedure

Polymerization was conducted in a 1-L round bottom, four-neck flask fitted with a mechanical stirrer, nitrogen inlet, condenser, and pipette outlet. The reactor was immersed in a thermostated water bath to maintain constant temperature. The appropriate amounts of water (a volume between 700 and 900 mL) and MMA were first introduced into the reactor and stirred under nitrogen atmosphere for 30 min. A specified amount of KPS dissolved in 40 mL of water was then added to the reactor, and the reaction was allowed to proceed at the selected polymerization temperature for 2 h. It was found that the rate of polymerization and the bead size are almost unchanged when the stirring speeds are in the range of 200–400 rpm. During the present study, the stirring speed was fixed at 300 rpm.

After given reaction times, the lattices were removed from the reactor in order to determine the monomer conversion, bead size, and average molecular weights. Solid polymers were separated from the lattices by cooling to  $-7^{\circ}\text{C}$  for at least 24 h and by precipitation using methanol as a nonsolvent. The fractional monomer conversion  $x$  was calculated as the amount of polymer formed per gram of the monomer present initially.

### Characterization

Scanning electron micrographs were obtained using a JEOL JSM-T330 electron microscope (SEM). Di-

lute samples (1–10 ppm) were prepared by placing a drop of the latex dispersion onto a brass surface and evaporating to dryness in a dust-free box at room temperature. The samples were then coated with gold, and scans were taken between  $0^{\circ}$  and  $45^{\circ}$  to the vertical. JEM-100 CX electron microscope was employed for transmission electron microscopy (TEM). The latex samples were diluted down to about 10 ppm, and one drop was placed onto a 20  $\mu\text{m}$  Formvar film-coated grid and allowed to air-dry at room temperature in a dust-free box. Measurement of the average particle diameters were performed using electron micrographs by sizing of at least 40 particles. Measurements were taken from different regions of all the electron micrographs. A standard deviation of 6% was found for the method of measurement. The  $z$ -average particle diameter and the particle size distribution were determined by a Malvern submicron particle size analyzer. Average particle diameters obtained from electron micrographs were found to be larger than those found by the particle size analyzer (see Table I).

Weight-average molecular weight and molecular weight distribution of polymers were obtained by size exclusion chromatography (Waters, Model M-6000A), equipped with refractive index detector, using two polystyrene gel columns (500 and 10,000 Å) at a flow rate of 1.0 mL/min in THF at  $40^{\circ}\text{C}$  and using polystyrene standards. The viscosity-average molecular weights were obtained from viscosity measurements in chloroform at  $20^{\circ}\text{C}$  with an Ubbelohde viscosimeter and using the Mark-Houwink constants<sup>12</sup>  $K = 0.0055 \text{ mL/g}$  and  $a = 0.79$ .

## RESULTS AND DISCUSSION

Homologous series of polymethyl methacrylate (PMMA) lattices were obtained allowing systematic variation of the temperature, monomer, initiator, and cross-linker concentrations, as well as the ionic strength of the aqueous phase. Synthesis conditions of the lattices are collected in Table I, together with their properties. Figure 1 illustrates the monodispersity in bead size from a typical polymerization of MMA. In the following sections, the effect of various reaction parameters on the kinetics of the emulsifier-free emulsion polymerization of MMA, as well as on the latex properties, is given.

### Polymerization Temperature

In Figure 2, fractional monomer conversion  $x$  versus time data are shown for different temperatures. The

Table I Synthesis Conditions and Properties of PMMA Latices<sup>a</sup>

Series	Run No.	Variable	D <sup>b</sup> (μm)	D <sub>z</sub> <sup>c</sup> (μm)	10 <sup>-6</sup> $\bar{M}_w$ <sup>d</sup>	10 <sup>-6</sup> $\bar{M}_v$ <sup>e</sup>	$\bar{M}_w/\bar{M}_n$ <sup>d</sup>
I	26 25 24 18	Temperature (°C)					
		60	0.28	0.26	1.1	1.1	60
		65	0.27	0.21	1.2	1.1	3.5
		70	0.24	0.19	0.85	0.97	1.52
IIa	17 16 15 14	[KPS] (×10 <sup>3</sup> /M)					
		0.25	—	0.14	1.2	1.4	1.2
		0.50	0.23	0.17	1.1	1.1	1.2
		1.00	0.23	—	0.83	0.78	1.44
IIb	4 6 11 2	[KPS] (×10 <sup>3</sup> /M)					
		1.50	0.24	0.15	0.7	0.61	1.66
		0.4	0.25	—	—	0.88	—
		0.7	0.21	—	—	0.66	—
III	20 19 18 15	[MMA] (M)					
		0.1	0.14	0.16	0.35	0.27	1.5
		0.2	—	0.20	0.68	0.67	1.6
		0.3	0.22	0.19	0.81	0.76	1.42
IVa	18 30 29 31	Ionic Strength KCl (mM)					
		0	0.22	0.19	0.81	0.76	1.42
		5	0.25	0.25	—	0.64	—
		10	0.30	0.30	—	0.61	—
IVb	18 33 32 34	NaCl (mM)					
		20	0.37	0.37	—	0.59	—
		0	0.22	0.19	0.81	0.76	1.42
		5	0.26	—	—	0.64	—
V	18 23 22 21	EGDM (Wt %)					
		10	0.32	—	—	0.58	—
		20	0.35	—	—	0.54	—
		0	0.22	0.19	0.81	0.76	1.42
	23 22 21	EGDM (Wt %)					
		5	0.22	0.14	—	—	—
		10	0.21	0.14	—	—	—
	21	15	0.18	0.13	—	—	—

<sup>a</sup> Polymerizations were carried out at 300 rpm for 2 h. The following conditions were fixed in each of the series. Series I: [MMA] = 0.3M; [KPS] = 1 × 10<sup>-3</sup>M. Series IIa: [MMA] = 0.4M; temperature = 75°C. Series IIb: [MMA] = 0.27M; temperature = 75°C. Series III: [KPS] = 1 × 10<sup>-3</sup>M; temperature = 75°C. Series IVa and IVb: [MMA] = 0.3M; [KPS] = 1 × 10<sup>-3</sup>M; temperature = 75°C. Series V: [MMA] = 0.3M; [KPS] = 1 × 10<sup>-3</sup>M; temperature = 75°C.

<sup>b</sup> Average particle diameters obtained from electron micrographs.

<sup>c</sup> z-Average particle diameters obtained from particle size analyzer.

<sup>d</sup> Weight-average molecular weight,  $\bar{M}_w$ , and polydispersity index,  $\bar{M}_w/\bar{M}_n$ , obtained by SEC using polystyrene standards.

<sup>e</sup> Viscosity-average molecular weight.

monomer and the initiator concentrations were 0.3 and 1 × 10<sup>-3</sup> M, respectively. As expected, the initial rate of polymerization increases with increasing temperature. Moreover, the limiting monomer conversions reached at low temperatures are much lower than 100%. This is due mainly to the formation of macroscopic agglomerates on the reactor wall and on the surface of the stirrer bar at temperatures below 70°C, which reduce the latex yield. Table I summarizes the average particle diameters and average

molecular weights of the polymers formed at different temperatures (series I). Increasing temperature decreases the size of the particles. This inverse dependence between the particle size and the polymerization temperature is due to the increasing decomposition rate of the initiator and increasing monomer solubility in the aqueous phase on raising temperature, which increase the concentration of growing chains and, thus, reduce the bead size. It must be noted, however, that an opposite effect of

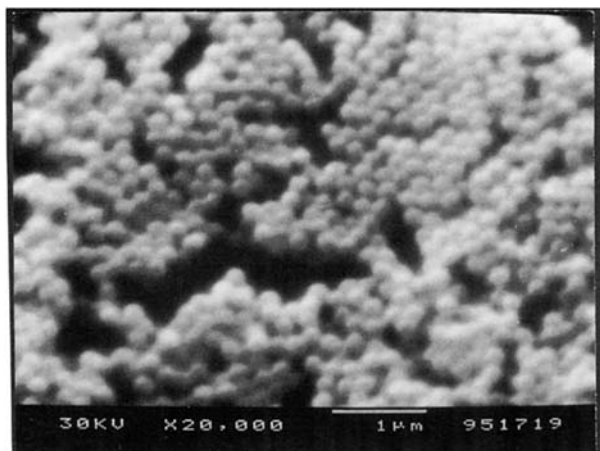


**Figure 1** PMMA beads prepared by emulsifier-free emulsion polymerization of MMA in the presence of potassium persulfate. Initial monomer concentration =  $0.3M$ .  $K_2S_2O_8$  concentration =  $1 \times 10^{-3}M$ , Polymerization temperature =  $75^\circ C$ . Scanning electron micrograph; magnification  $20,000\times$ .

the polymerization temperature on the bead size may also be expected in MMA polymerization<sup>6</sup>; namely, since increasing temperature increases the water solubility of MMA and, so, increases the critical chain length for polymer precipitation, increasing temperature may lead larger particles. According to the experimental results, we can conclude that the second effect of temperature is insignificant compared to the predominant role of the initiated chain concentration in determining the particle size.

Particle size distribution of lattices formed at different temperatures is shown in Figure 3. It can be seen that the reduction of the average bead size on raising temperature is accompanied with the formation of particles with narrower size distribution. Thus, at low temperatures, the number of sulfate ions seems to be insufficient to stabilize the particles formed. Temperatures as high as  $70^\circ C$  are necessary to obtain stable and, thus, monodisperse PMMA lattices.

The weight-average molecular weights and molecular weight distributions were determined by size exclusion chromatography (SEC) based on polystyrene standards. The average molecular weights and the polydispersities shown in Table I (Series I) indicate that polymerization at temperatures higher than  $70^\circ C$  gives polymers having relatively narrow molecular weight distributions. Polydispersity index approaches 1.4 with increasing temperature. However, as the temperature decreases, molecular weight distribution of polymers becomes broader. The SEC chromatogram of the polymers prepared below  $70^\circ C$

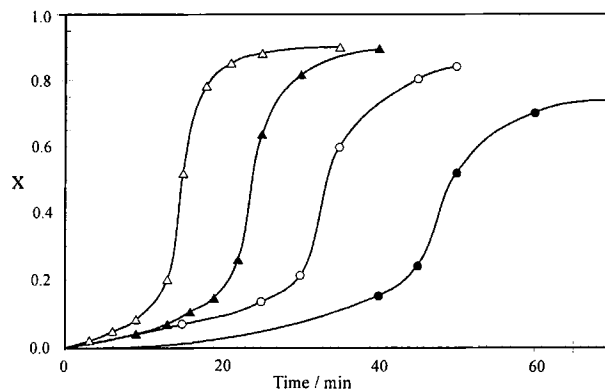


**Figure 2** Variation of the fractional monomer conversion  $x$  versus time histories in emulsifier-free emulsion polymerization of MMA with the polymerization temperature. Initial monomer concentration =  $0.3M$ .  $K_2S_2O_8$  concentration =  $1 \times 10^{-3}M$ , Polymerization temperature =  $60^\circ C$  (●),  $65^\circ C$  (○),  $70^\circ C$  (▲), and  $75^\circ C$  (△).

shows a pronounced low molecular weight tail, as seen in Figure 4. Since the probability of the radical entry into the particles and, thus, the lifetime of a growing chain depend on the particle size, broad particle size distribution would necessarily lead to the formation of polymers having broad molecular weight distribution, as was found experimentally at low temperatures. Thus, the experimental data indicate a direct correlation between the distributions of particle size and polymer molecular weight. It must be pointed out that the kinetic conclusions made above base on the experimental data obtained at temperatures above  $60^\circ C$ . This is due to the formation of significant amounts of coagulum at low temperatures.

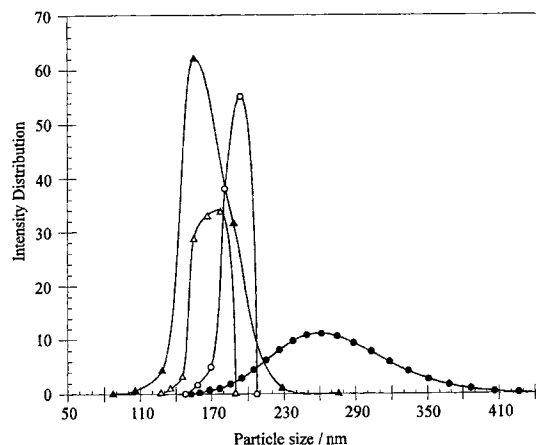


**Figure 3** Dependence of the particle size distribution of the lattices on the polymerization temperature. See Figure 2 caption for the reaction conditions. Polymerization temperature =  $60^\circ C$  (●),  $65^\circ C$  (○),  $70^\circ C$  (▲), and  $75^\circ C$  (△).

### Initiator and Monomer Concentrations

In this section, the polymerization temperature was held constant at 75°C, and the concentrations of the initiator potassium persulfate (KPS) and the monomer MMA were varied. In Figures 5 and 6, conversion versus time plots are shown for different KPS and MMA concentrations, respectively. The rate of polymerization increases as the concentration of KPS increases or that of MMA decreases. Since increasing initiator or decreasing monomer concentration increases the radical to monomer mole ratio, this trend is expected. Moreover, the polymerization carried out at 0.1M MMA concentration shows an acceleration in polymerization rate starting right down to zero conversion; i.e., the interval *I* was not detected for this monomer concentration. This could be due to lack of data for  $x < 0.2$ , as seen in Figure 6, or, due to the complete solubility of the monomer in the aqueous phase and start of the polymerization in a homogeneous manner. Indeed, the aqueous solubility of MMA, which is reported to be<sup>8</sup> 0.16 mol/L, is close to the initial MMA concentration of this polymerization system.

The average particle sizes of the lattices and polymer molecular weights for different concentrations of KPS and MMA are collected in Table I (Series II and III, respectively). The particle size does not change much with the initiator concentration and increases slightly with increasing monomer concentration. The polydispersities of the resulting polymers range from 1.2 to 1.7 and relatively narrow molecular weight distributions were obtained at low initiator concentrations. In order to explain the experimental findings, it should be borne in mind that the initiator concentration has two opposite effects on the bead size in emulsion polymerization. First,

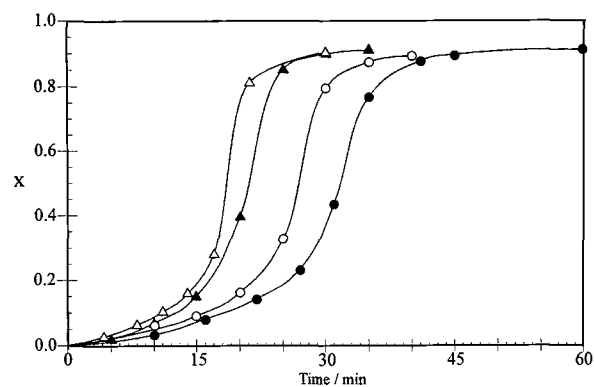


**Figure 5** Variation of the conversion  $x$  versus time histories with the initiator concentration. Initial monomer concentration = 0.4M. Polymerization temperature = 75°C.  $[K_2S_2O_8] \times 10^3 = 0.25$  (●), 0.50 (○), 1.00 (▲), and 1.50M (△).

increasing KPS concentration increases the number of sulfate ions involved in stabilization of the particles leading to smaller particles. Second, increase in KPS concentration also increases the ionic strength of the aqueous phase, which results larger particles. Thus, it seems that the two opposite effects of the initiator KPS compensate each other under the experimental conditions. Furthermore, reduced particle diameter with decreasing monomer concentration is due to the limitation of the growth of particles during polymerization.

According to the experimental results, the distribution of the molecular weights broadens as the initiator concentration increases (Table I). This is also an indication of the increased instability of the particles due to the increased ionic strength of the aqueous phase on raising KPS concentration, which accelerates the agglomeration processes. Thus, par-

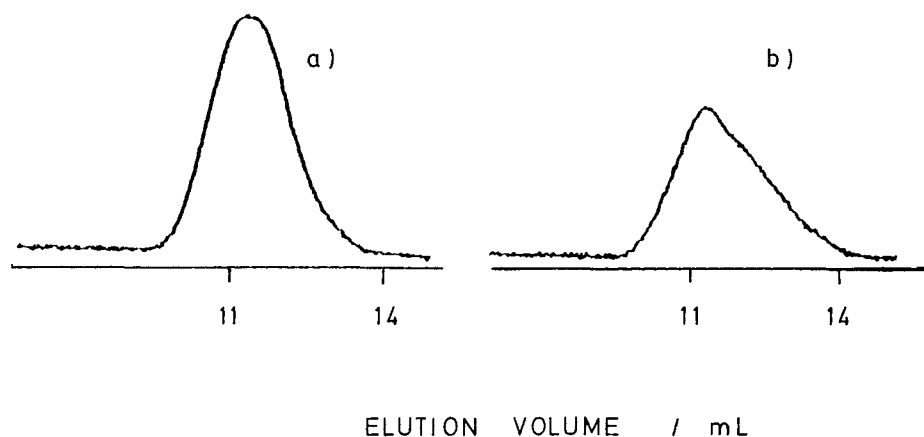


**Figure 4** SEC chromatograms of PMMA prepared at 75 (a) and 60°C (b). See Figure 2 caption for the reaction conditions.

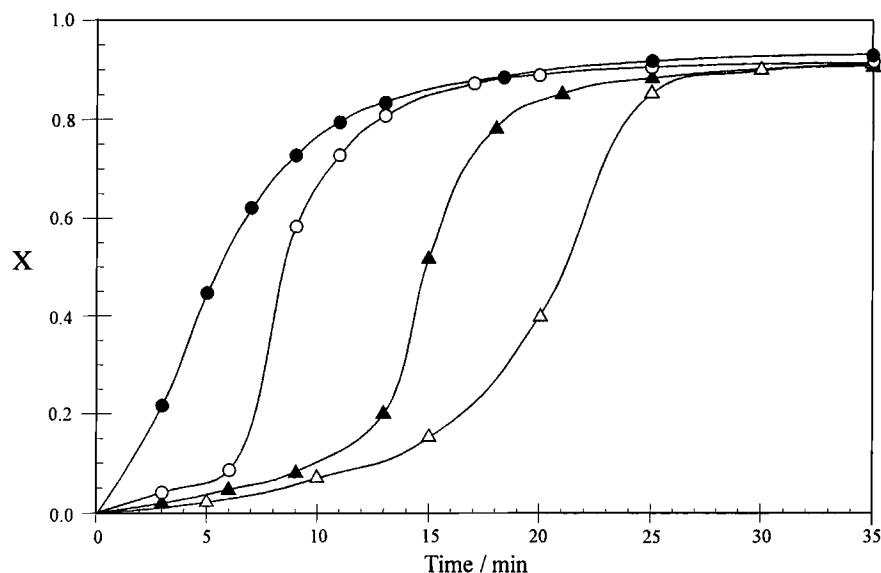


**Figure 6** Variation of the conversion  $x$  versus time histories with the monomer concentration.  $K_2S_2O_8$  concentration =  $1 \times 10^{-3}M$ . Polymerization temperature =  $75^\circ C$ .  $[MMA]$  = 0.1 (●), 0.2 (○), 0.3 (▲), and 0.4M (△).

ticle coagulation is more pronounced at high initiator concentrations yielding broader distributions of particle size and polymer molecular weight.

The particle diameters collected in series I–III in Table I indicate that they change only slightly depending on the reaction conditions. This may reflect particle formation by the agglomeration of primary particles. Thus, following primary nucleation by precipitation of growing chains, agglomeration and particle coalescence occur and fix the number of beads nucleated.

### Ionic Strength

The ionic strength was generated by contributions from a constant initiator concentration ( $1 \times 10^{-3}M$ ) and added strong electrolytes KCl or NaCl. Time conversion curves at different ionic strengths generated using KCl are shown in Figure 7. Increasing KCl concentration increases the duration of interval  $I$  of the polymerization by reducing the initial rates. This is due to the salting out effect of KCl, which reduces the water solubility of MMA and, thus, decreases the rate of polymerization in the aqueous phase. Figure 8 is a plot of the average particle diameter against the ionic strength. The error bars represent the standard deviations of the measurements. The size of the particles increases linearly with increasing ionic strength of the aqueous phase. As seen in Table I (Series IV), final particle diameter varies between 0.22 and  $0.37 \mu m$ , depending

on the salt concentration. Thus, the ionic strength of the aqueous phase has a dominant effect on particle diameter and can easily be controlled by varying the salt concentration of the aqueous phase.

Another point shown in Table I is that the molecular weight of the polymers decreases as the ionic strength of the aqueous phase increases. This feature is better seen in Figure 9, which illustrates the dependence of the viscosity-average molecular weight  $M_v$  on the salt concentration of the aqueous phase. One may expect that the increased bead size with increasing salt concentration increases the probability of radical entry into the growing particles and, so, leads to shorter kinetic chains.

### EGDM Concentration

Emulsion polymerization containing divinyl monomers produces microgel particles having pendant vinyl groups on their surfaces.<sup>13</sup> It was shown that in conventional emulsion polymerization of divinyl monomers, more and smaller particles are produced than in the case of monovinyl monomers under the same conditions.<sup>14–16</sup> Figure 10 shows the effect of the EGDM concentration on the rate of polymerization in MMA polymerization. Addition of EGDM as a cross-link agent increases the polymerization rate significantly. Since the reactivities of the vinyl groups on MMA and EGDM monomers are almost equal,<sup>17</sup> the enhancement in the rate of polymerization indicates diffusion controlled termination due

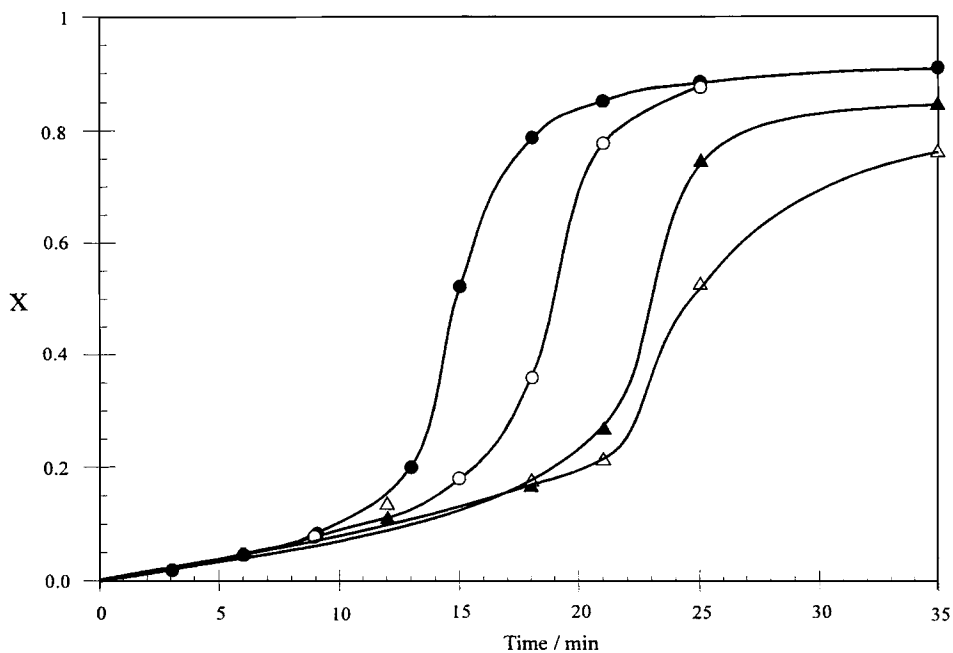


**Figure 7** Variation of the conversion  $x$  versus time histories with the ionic strength of the aqueous phase generated by KCl addition. MMA concentration =  $0.3M$ .  $K_2S_2O_8$  concentration =  $1 \times 10^{-3}M$ . Polymerization temperature =  $75^\circ C$ .  $[KCl] = 0$  (●),  $5$  (○),  $10$  (▲), and  $20$  mM (△).

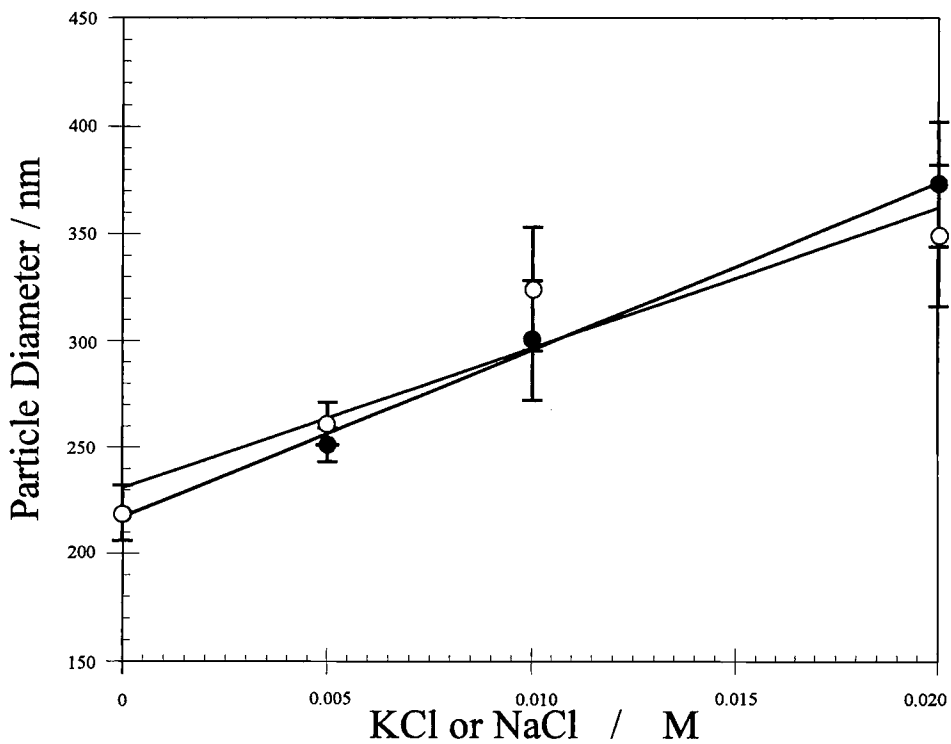


**Figure 8** Variation of the average particle size with the ionic strength. The ionic strength is generated using KCl (●) and NaCl addition (○). See Figure 7 caption for the reaction conditions.

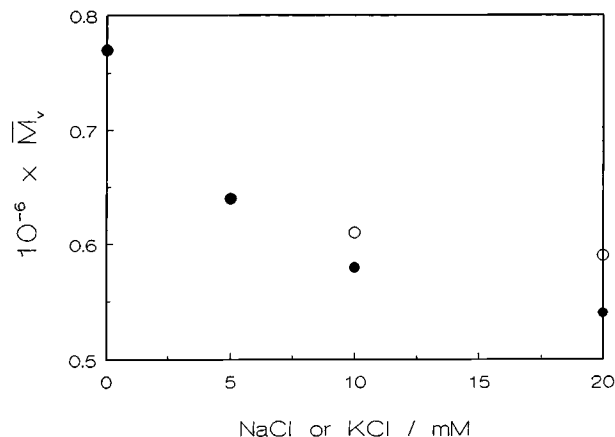


**Figure 9** Dependence of the viscosity-average molecular weight of PMMA,  $\bar{M}_v$ , on the ionic strength of the aqueous phase in terms of the concentrations of NaCl (●) or KCl (○). See Figure 7 for the reaction conditions.

to the gel effect in the cross-linking system. Similar behavior was also observed previously in homogeneous polymerization system.<sup>18,19</sup> Furthermore, as seen in Table I (series V), the particle size decreases as the concentration of the cross-linker increases. The effect of the cross-linker on particle size seems to be similar to that of the decreased monomer concentration; in cross-linking polymerization, the bead growth is limited due to the reduced swellability of the cross-linked particles. Figure 11 shows the particle size distribution of lattices obtained at different cross-linker concentrations. Addition of cross-linker clearly increases the degree of uniformity of parti-

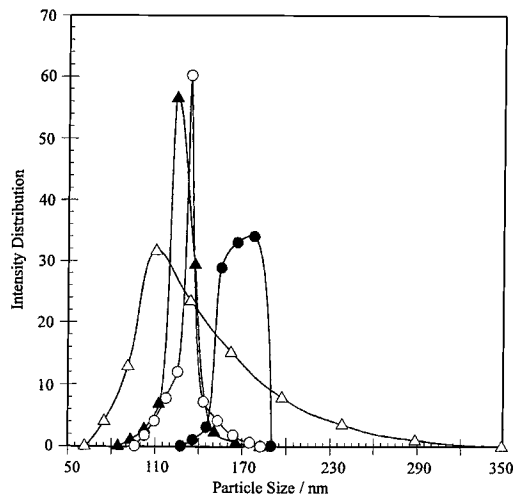


**Figure 11** Dependence of the particle size distribution of the lattices on the EGDM concentration. See Figure 9 caption for the reaction conditions. EGDM = 0 (●), 5 (○), 10 (▲), and 15 wt % (△).

cles. However, at high EGDM contents, agglomeration through the pendant vinyl groups on the surface of the particles may lead to broadening of the size distribution.

## CONCLUSIONS

Emulsifier-free emulsion polymerization of MMA was carried out using KPS as an initiator of the polymerization and also as a stabilizer of the growing

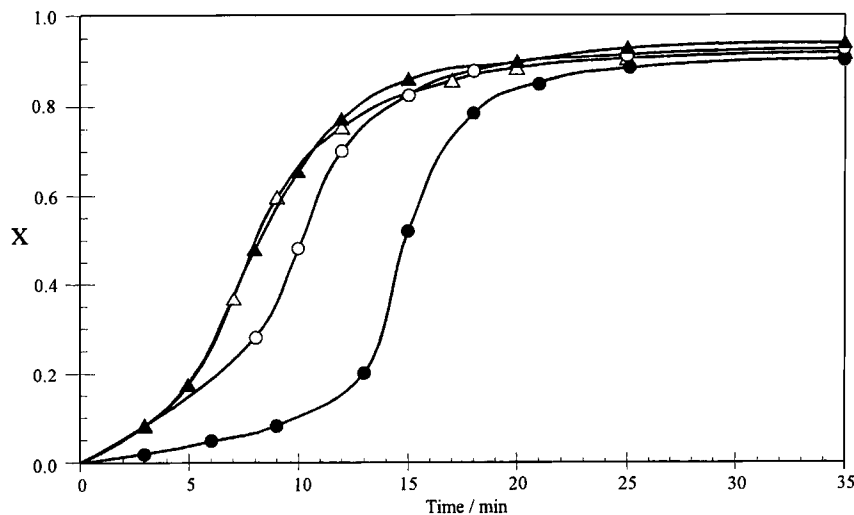


**Figure 10** Variation of the conversion  $x$  versus time histories with the EGDM concentration. MMA concentration = 0.3M.  $K_2S_2O_8$  concentration =  $1 \times 10^{-3}M$ . Polymerization temperature = 75°C. EGDM = 0 (●), 5 (○), 10 (▲), and 15 wt % with respect to MMA monomer (△).

particles. Monodisperse PMMA lattices with particle diameters varying between 0.14–0.37  $\mu\text{m}$  and polymer molecular weights of the order  $0.4 \times 10^6$  to  $1.2 \times 10^6$  g/mol were prepared. The initial rate of polymerization increases with increasing temperature, KPS-MMA mole ratio, EGDM content, or with decreasing ionic strength of the aqueous phase. A reasonably linear correlation is observed between the particle diameter and the ionic strength of the aqueous phase. Thus, the particle diameter, as well as the polymer molecular weight, can be controlled easily by the ionic strength of the aqueous phase. It was also shown that the particle size can be limited by reducing the monomer concentration or by using the cross-linking agent EGDM. The uniformity of the latex particles increases as the temperature increases or the initiator concentration decreases.

## REFERENCES

1. T. Matsumoto and A. Ochi, *Kobunshi Kagaku*, **22**, 481 (1965).
2. A. R. Goodall, M. C. Wilkinson, and J. Hearn, *J. Polym. Sci., Polym. Chem. Ed.*, **15**, 2193 (1977).
3. J. Hearn, M. C. Wilkinson, A. R. Goodall, and M. Chainey, *J. Polym. Sci., Polym. Chem. Ed.*, **23**, 1869 (1985).
4. Z. Song and G. W. Poehlein, *J. Polym. Sci., Polym. Chem. Ed.*, **28**, 2359 (1990).
5. D. Zou, V. Derlich, K. Gandhi, M. Park, L. Sun, D. Kriz, Y. D. Lee, G. Kim, J. J. Aklonis, and R. Salovey, *J. Polym. Sci., Polym. Chem. Ed.*, **28**, 1909 (1990).
6. D. Zou, S. Ma, R. Guan, M. Park, L. Sun, J. J. Aklonis, and R. Salovey, *J. Polym. Sci., Polym. Chem. Ed.*, **30**, 137 (1992).
7. G. T. D. Shouldice, G. A. Vandezande, and A. Rudin, *Eur. Polym. J.*, **30**, 179 (1994).
8. Z. Song and G. W. Poehlein, *J. Colloid Interface Sci.*, **128**, 486 (1989).
9. Z. Song and G. W. Poehlein, *J. Colloid Interface Sci.*, **128**, 501 (1989).
10. R. M. Fitch and C. H. Tsai, in *Polymer Colloids*, R. M. Fitch, Ed., Plenum, New York, 1971, p. 73.
11. M. Arai, K. Arai, and S. Saito, *J. Polym. Sci., Polym. Chem. Ed.*, **18**, 2811 (1980).
12. J. Brandrup and E. H. Immergut, *Polymer Handbook*, 2nd ed., Wiley, New York, 1974, pp. IV–13.
13. W. Funke, H. Bauer, B. Joos, J. Kaczun, B. Kleiner, U. Leibelt, and O. Okay, *Polymer Int.*, **30**, 519 (1993).
14. W. Obrecht, U. Seitz, and W. Funke, ACS Symposium Series, Number 24, Emulsion Polymerization, I. Piirma and J. L. Gardon, Eds., American Chemical Society, Washington, D.C., 1976, p. 92.
15. I. Capek, J. Kostrubova, and J. Barton, *Macromol. Chem., Macromol. Symp.*, **31**, 213 (1990).
16. I. Capek and P. Potisk, *Polym. J.*, **24**, 1037 (1992).
17. R. S. Whitney and W. Burchard, *Makromol. Chem.*, **181**, 869 (1980).
18. O. Okay and H. J. Naghash, *Polym. Bull.*, **33**, 665 (1994).
19. O. Okay, H. J. Naghash, and I. Capek, *Polymer*, **35**, 2613 (1995).

Received October 3, 1995

Accepted February 5, 1996